ORIGINAL PAPER

Hydrogeochemical Processes Controlling the Water Chemistry of a Closed Saline Lake Located in Sahara Desert: Lake Qarun, Egypt

Mahmoud S. M. Abdel Wahed · Essam A. Mohamed · Mohamed I. El-Sayed · Adel M'nif · Mika Sillanpää

Abstract We present here the first detailed hydrogeochemical study about Lake Qarun. It is a closed, saline, and alkaline lake located in the North African Sahara Desert. It has no outflow except by evaporation. This lake is the deepest area in the Fayoum Depression with elevation 43 m below sea level. In this area, Nile River is the main source of water and Lake Qarun acts as the main reservoir of all drainage waters. Along the flow path of water, the salinity of water increases with increasing proximity to Lake Qarun and the water chemistry has developed from Ca–Mg–HCO$_3$ at head waters to Na–Cl–SO$_4$ in low lands and in Lake Qarun. The main processes that control the water chemistry in the studied area are dissolution of soluble salts along with continuous evapoconcentration. The progressive evaporation of drainage water inflow has increased the concentrations of Na, Mg, Cl, and SO$_4$ in Lake Qarun water, while Ca and HCO$_3$ have been depleted through CaCO$_3$ precipitation. This is confirmed by the application of Hardie and Eugster's model parallel with a PHREEQC simulated evaporation model. Both models demonstrated that the evolution of lake water during evaporation should reach the final composition of "Na–Mg–SO$_4$–Cl." Oxygen isotope (δ^{18}O) values of the studied water samples showed a strong positive correlation with electrical conductivity values supporting the effect of evapoconcentration process on the evolution of the lake brine. This study presented an integrated geochemical approach that can help in understanding similar cases studies in arid environments.

M. S. M. Abdel Wahed (✉) · M. Sillanpää
Laboratory of Green Chemistry, LUT Chemistry Department, Lappeenranta University of Technology, Sammonkatu 12, 50130 Mikkeli, Finland
e-mail: m.abdelwahed80@yahoo.com; mahmoud.abdel-wahed@lut.fi

M. S. M. Abdel Wahed · E. A. Mohamed · M. I. El-Sayed
Geology Department, Faculty of Science, Beni-Suef University, Beni Suef, Egypt

A. M'nif
Centre National de Recherche en Sciences des Matériaux, Technopole Borj Cedria, B.P. 73, 8027 Soliman, Tunisia

1 Introduction

In a closed hydrological system, the composition of concentrated lake brines largely depends on labile lithologies that are leached and altered by inflow waters in the drainage basin surrounding a salt lake (Eugster 1980; Hardie and Eugster 1970). Closed lakes are exclusive features of the arid and semiarid zones where they are salty with variable degrees of salinity.

Lake Qarun, the object of the present investigation, is one of the largest inland lakes in the North African Sahara Desert. The lake water is alkaline with pH values between 8.0 and 8.7, and saline with average total dissolved salts (TDS) of 36 g/L. The lake level is at ≈ 43 m below sea level, which makes it the deepest area in the Nile River flood plain and in the Fayoum Depression (Figs. 1, 2). It is one of oldest lakes in Egypt. A full historical background and a summary of past environmental changes for the lake may be found in the scientific literatures (e.g., Ball 1939; Flower et al. 2006; Meshal 1977). The lake is surrounded by cultivated lands on its southern and south eastern sides which slope sharply toward the lake. This provides a natural aid forming a drainage water disposal site from the cultivated lands of the whole Depression of Fayoum. The agriculture drainage water annually carries 470×10^6 kg of dissolved salts into Lake Qarun (Rasmy and Estefan 1983). The evolution of the lake water chemistry is mainly based on the chemical composition of the inflow drainage waters. Because the lake has no outlet and the climatic
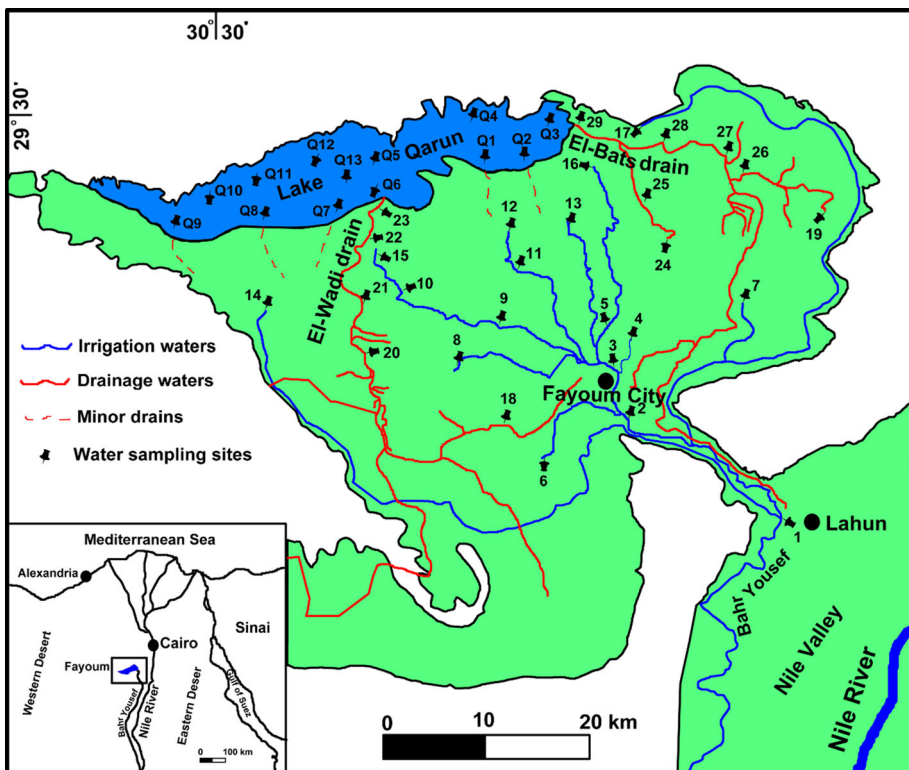
Fig. 1 Location map of the Fayoum area, showing the sampling sites of the studied water samples
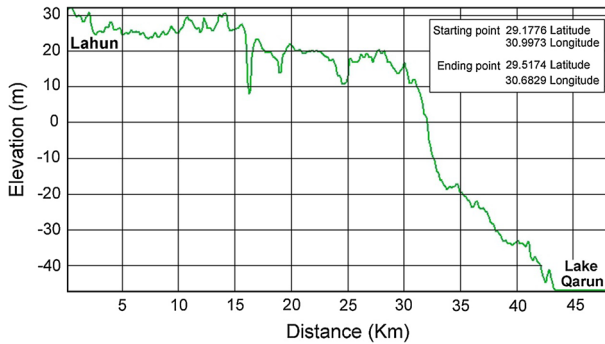
Fig. 2 Cross section illustrates the land slope from Lahun to Lake Qarun

conditions are warm and dry almost all the year, the lake brine gradually evaporates and its salinity increases. As a result, the lake has undergone marked salinization with accompanying changes in aquatic biota (Flower et al. 2006).

The objectives of the present work are mainly focused on the following:

1. Study in details the geochemical evolution of the surface water in the Fayoum Depression through its flow path from Nile at Lahun toward Lake Qarun (Fig. 1).
2. Identification the geochemical processes controlling the surface water chemistry in the Fayoum Depression.
3. Deduce a detailed geochemical model that demonstrates the evolution of Lake Qarun water.
4. Carry out a simulated evaporation model of Lake Qarun water to study the geochemical changes expected by further evaporation of lake water, assuming that the lake has no outflow except by evaporation.

2 Study Area and Methods

2.1 Site Description

Lake Qarun is located between the longitudes of 30°24′ & 30°49′E and latitudes of 29°24′ & 29°33′N, about 95 km south west of Cairo (Fig. 1). The lake has an irregular elongated shape of about 45 km length and 5.7 km mean width with an average area of about 240 km^2. The average depth of the lake is approximately 4.2 m. The deepest region (≈ 8 m) is located in the middle of the lake while shallowest region lies in the eastern portion of the lake. Nearly 67 % of the lake area is between the 2 and 5 m depth contours, while only 18 % of the lake area is deeper than 5 m (Baioumy et al. 2010).

Nile River, the main source of fresh water, is reaching the Fayoum region via the Bahr Yousef channel (Fig. 1). Agricultural returns have been collected as drainage water and passed into Lake Qarun through two main drains, El-Wadi and El-Bats, with other minor drains between them (Fig. 1). To the north, the area is completely covered by sand and rock with several exposures of diatomite. This landscape is not irrigated and is virtually devoid of vegetation.

2.2 Climate

The studied catchment lies in Egypt's arid belt with a hot, long dry summer and a mild short winter, and consequently, the climate is generally warm and dry (Baioumy et al. 2010). In addition, it is characterized by low seasonal rainfall and a high evaporation rate. Rainfall is extremely low at <10 mm annually (Flower et al. 2006). The lowest evaporation rate (1.9 mm/day) is recorded in January while the highest value (7.3 mm/day) is recorded in June and the annual mean relative humidity varies between 50 and 62 % (Ali and Abdel Kawy 2013).

2.3 Hydrology

The irrigation and agricultural system in the Fayoum region depends mainly on Nile water. Fayoum City (Fig. 1), the principal town in the area, is a water distribution center for the Fayoum (domestic demands), and a network of canals and small pumping stations deliver water to the agricultural regions. Lake Qarun is a natural sink for drainage water from this area as it is surrounded from the south and southeast by cultivated land which slopes steeply toward the lake (Figs. 1, 2). Drainage waters are passed to Lake Qarun through two principal drains named El-Wadi and El-Bats drains (Fig. 1). The lake receives drainage water with a volume of about 338×10^6 m^3/year from El-Bats and El-Wadi drains in addition to about 67.8×10^6 m^3/year from groundwater while it losses about 415×10^6 m^3/year by evaporation (El-Shabrawy and Dumont 2009; Meshal 1977). The lake itself has no outflow except by evaporation (Meshal 1977; Wolters et al. 1989).

2.4 Geology and Geomorphology

Fayoum is a natural depression in the Western Desert of Egypt, extending over 6,068 km^2. Tableland areas surround the Fayoum Depression from the east, west, and south separating it from neighboring depressions, the Nile valley, and Wadi El Rayan. Most of the cultivated soils in the Fayoum Depression are deep alluvial loam or clayey, derived mainly from the Nile flood alluvium. The Fayoum Depression has a dense net of irrigation canals and drains. The Fayoum Depression area includes three main landscapes, i.e., lacustrine plain, alluvial–lacustrine plain, and alluvial plain (Abdel Kawy and Belal 2013; Ali and Abdel Kawy 2013). The southern shore of Lake Qarun is mostly surrounded by lacustrine deposits. These deposits cover an area of 198 km^2 and are classified as highly saline and poor productivity soils (Abdel Kawy and Belal 2013). The current status of soil salinity, sodicity, and water table indicate that most lacustrine and alluvial–lacustrine soils in the Fayoum Depression are actually being degraded by salinization, sodification, and water-logging (Ali and Abdel Kawy 2013).

Geologically, the stratigraphic sequence in the area ranges in age from Quaternary to Tertiary (Fig. 3). The Fayoum Depression itself is excavated in Middle Eocene rocks, which composed essentially of gyps-ferrous shale, white marls, limestone, and sand (Hammad et al. 1983; Said 1993). The Quaternary deposits are widely distributed over the Fayoum area in the form of eolian, Nilotic (alluvial sediments), and lacustrine deposits. The alluvial sediments are composed of sands and gravels of variable sizes intercalated with calcareous silt and clay contents (Tamer 1968). The lacustrine deposits include claystone, gypsum, and calcareous materials intercalated with ferruginous sandy silt (Metwaly et al. 2010). The lacustrine deposits have prevailed in the area and extend to the south of Lake Qarun. In the whole area, Quaternary sediments directly overlay the limestone deposits of the Eocene age.
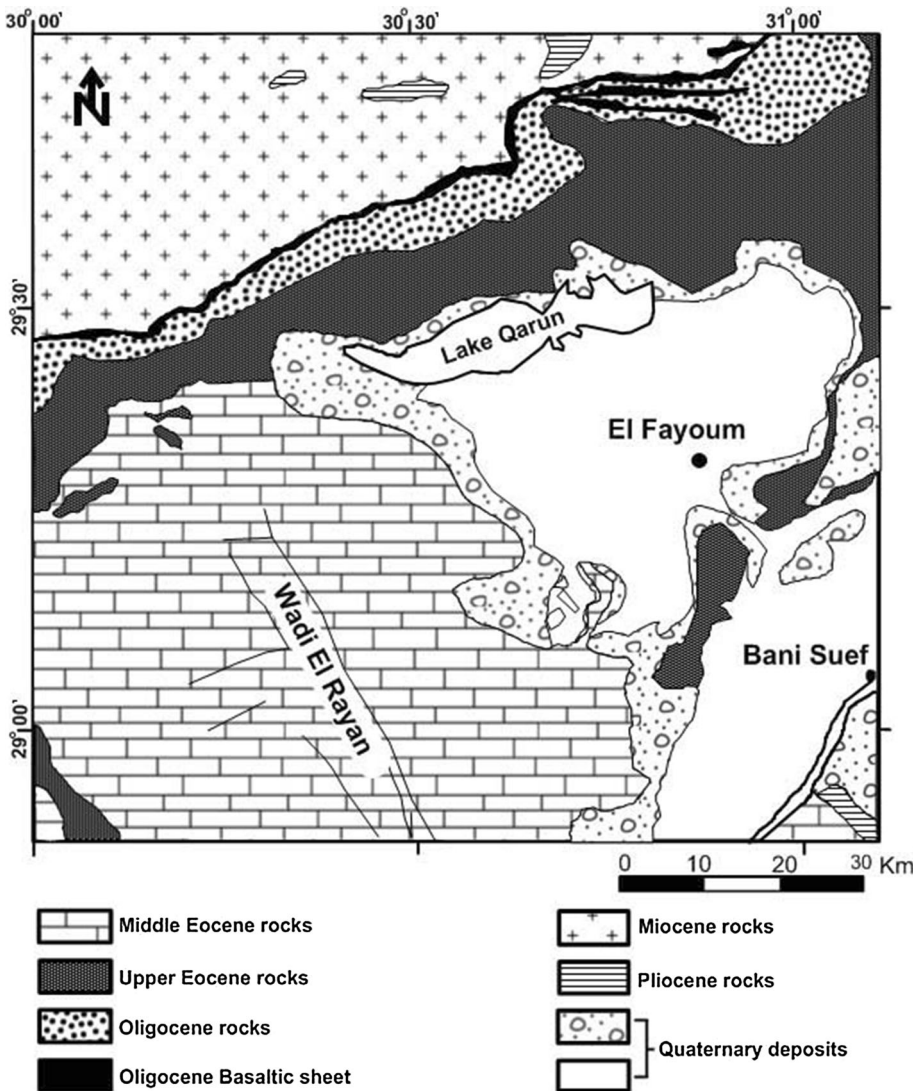
Fig. 3 Geological map of Fayoum area

2.5 Sampling and Sample Analysis

In June 2010, 2011, and 2012, surface water samples at Lake Qarun were collected regularly from 13 sites (Q1–Q13). In June 2012, additional surface water samples from irrigation canals and the drainage network were collected from 29 sites (samples 1–29) (Fig. 1). All samples were analyzed for sodium (Na^+), calcium (Ca^{2+}), magnesium (Mg^{2+}), potassium (K^+), sulfate (SO_4^{2-}), chloride (Cl^-), bicarbonate (HCO_3^-), silica (SiO_2) and oxygen isotopes ($\delta^{18}O$). At all sampling locations, GPS coordinates were recorded. Measurements of electrical conductivity (EC), pH, and temperature were carried out in the field using a SG78-SevenGo Duo pro (pH/Ion/Conductivity) portable meter with

an accuracy ±0.002 pH units, ±0.5 % of full-scale EC, and ±0.1 °C for temperature. After in situ measurements, the water samples for major ions analysis were filtered through a 0.45-μm disposable cellulose acetate syringe membrane filter (33 mm diameter, white rim, Whatman GmbH, Germany). The filtered samples were transferred into preacid-washed polyethylene (PE) containers which divided into three portions: (1) water samples acidified to pH <2 for main cations analysis; (2) water samples for main anion analysis; and (3) water samples for oxygen isotopes analysis. All sampling containers were left to dry for 2 days after acid or deionized washing. The PE bottles were filled without air bubbles and tightly capped immediately with PE screw caps. Then, the water samples were stored in double PE plastic bags, kept at 4 °C, and transported to the laboratory as soon as possible after sampling. Analysis of HCO_3^- was conducted immediately after samples reached the laboratory and the remaining analyses within the next 24 h. Total dissolved solids (TDS) were calculated using the sum of the major ions (Na^+, K^+, Ca^{2+}, Mg^{2+}, HCO_3^-, SO_4^{2-}, Cl^-, and SiO_2), assuming that the fraction below 0.45 μm can be considered "dissolved." All analyses, except $\delta^{18}O$, were carried out at the Water Quality Central Laboratory, Fayoum Drinking Water and Sanitation Company, Fayoum, Egypt. The analyses were done in accordance with approved analytic methods (APHA 1998) as summarized in Table 1. All analytical procedures are accredited according to ISO/IEC 17025.

Water samples were analyzed for oxygen isotope composition ($\delta^{18}O$) using a Gas Bench II system (Thermo Finnigan, Bremen, Germany) coupled with a Thermo Finnigan Delta plus XP isotope ratio mass spectrometer in the stable isopologues laboratory at McMaster University, Canada. The details of the analytical procedures are described in Klein Gebbinck et al. (2014).

All oxygen isotope results were obtained by calculating the mean of the last 10 measurements and normalized by using two inter-laboratory water standards (i.e., MRSI-1 and MRSI-2). The δ18O values of the samples were reported normalized to V-SMOW, and the precision for replicate sample analyses is ≤0.08 ‰.

Saturation indices (SI) of the dissolved minerals in water samples were calculated using the PHREEQC version 3 software (PHREEQC-3) (Parkhurst and Appelo 2013). In addition, a simulated evaporation model of Lake Qarun water was carried out also using PHREEQC-3 software. This software was compiled on March 13, 2014. It is a computer program that is designed to perform a wide variety of aqueous geochemical calculations. One of the new features of the PHREEQC version 3 is the Pitzer aqueous model (Pitzer database), which can be used for high-salinity waters that are beyond the range of application for the Debye-Hückel theory (Parkhurst and Appelo 2013).

Table 1 Analytical methods of the studied water samples, after APHA (1998)

Analytical parameters	Method (APHA 1998)	Uncertainty (%)
SO_4^{2-}	4500-SO_4^{2-} E	12.9
Cl^-	4500-Cl^- B	4.1
HCO_3^-	2320-B Titration method	1.8
Na^+	3120 B, ICP method by ICP-OES	3.6
K^+	3120 B, ICP method by ICP-OES	5
Mg^{2+}	3120 B, ICP method by ICP-OES	11.6
Ca^{2+}	3120 B, ICP method by ICP-OES	9
SiO_2	4500-SiO_2 C	8.7

Table 2 General parameters and major ion chemistry of the surface waters in Fayoum Depression, Egypt

Water system	Sampling sites	pH	EC	Ca^{2+}	Mg^{2+}	Na^+	K^+	HCO_3^-	SO_4^{2-}	Cl^-	SiO_2	TDS	$\delta^{18}O^b$
Irrigation waters	1	7.70	0.38	36.16	9.43	19.78	3.21	120.00	38.20	23.18	5.11	255.07	+3.09
	2	7.70	0.45	36.10	10.60	30.20	3.90	132.80	52.32	37.68	5.06	308.66	+3.12
	3	7.70	0.39	36.20	9.89	19.58	3.04	122.80	39.90	25.75	4.73	261.89	+3.21
	4	7.60	0.44	31.90	9.30	22.00	3.90	128.80	51.90	33.79	4.53	286.12	+3.19
	5	7.80	0.42	38.10	10.30	22.40	3.31	122.40	47.80	28.72	6.23	279.26	+3.22
	6	7.60	0.40	34.00	9.90	24.70	3.80	136.80	39.43	25.38	5.07	279.08	+3.22
	7	7.53	0.45	37.10	10.80	38.40	4.30	135.60	48.50	33.72	5.98	314.40	+3.13
	8	7.50	0.50	37.70	11.60	35.80	4.50	144.80	56.90	39.32	5.71	336.33	+3.26
	9	7.60	0.36	32.10	9.60	21.90	3.80	130.80	28.90	16.68	4.74	248.52	+3.19
	10	7.60	0.65	43.30	16.16	47.20	8.22	165.20	72.70	56.06	10.60	419.44	+3.33
	11	7.50	0.68	46.32	15.22	45.20	4.72	174.00	75.90	61.60	9.87	432.83	+3.24
	12	7.50	0.76	47.91	15.96	46.10	5.17	182.40	73.34	57.10	10.73	438.71	+3.27
	13	7.77	0.87	54.20	19.79	71.40	5.53	184.80	118.00	82.20	11.82	547.74	+3.30
	14	7.50	0.60	46.32	15.22	45.20	4.72	174.00	75.90	61.60	9.87	432.83	+3.24
	15	7.50	0.91	47.91	15.96	46.10	5.17	182.40	73.34	57.10	10.73	438.71	+3.27
	16	7.90	1.11	62.00	20.49	100.10	6.13	173.20	154.90	151.10	8.62	676.54	+3.37
	17	7.70	3.76	144.40	37.73	506.20	39.10	212.40	593.60	807.80	9.14	2,350.37	+4.22
Drainage waters	18	7.50	1.01	49.20	19.30	112.60	7.00	198.80	147.80	116.96	8.87	660.53	+3.39
	19	7.60	0.97	73.27	15.73	85.50	6.13	154.00	154.10	119.28	8.53	616.54	+3.49
	20	7.60	1.38	77.90	23.49	139.60	7.78	183.20	207.90	190.30	12.47	842.64	+3.56
	21	7.60	1.60	93.09	26.55	142.40	8.67	192.80	276.80	241.50	14.15	995.96	+3.57
	22	7.80	1.73	100.20	28.60	156.50	6.95	204.40	292.30	260.50	14.69	1,064.14	+3.62
	23[a]	7.70	1.84	188.00	65.89	481.60	17.10	277.50	510.30	730.30	12.61	2,283.30	+3.62
	24	7.50	1.10	53.33	22.20	117.20	8.63	224.40	141.60	116.47	10.84	694.67	+3.24
	25	7.70	1.91	82.30	32.51	182.40	15.10	295.20	291.10	303.90	15.14	1,217.65	+3.34

Table 2 continued

Water system	Sampling sites	pH	EC	Ca^{2+}	Mg^{2+}	Na^+	K^+	HCO_3^-	SO_4^{2-}	Cl^-	SiO_2	TDS	$\delta^{18}O$[b]
	26	7.60	1.98	120.00	27.58	204.90	10.25	190.80	380.80	308.60	13.26	1,256.19	+3.61
	27	7.50	1.94	106.30	26.56	193.80	10.49	196.00	361.60	308.60	13.52	1,216.87	+3.49
	28	7.50	2.10	106.00	30.52	203.30	11.90	186.40	393.30	332.14	11.72	1,275.28	+3.48
	29[a]	7.50	2.40	166.80	63.60	425.00	23.30	220.10	502.00	758.30	13.14	2,172.24	+3.50
Lake Qarun waters[a]	Q1	8.20	34.10	418.80	969.87	9,360.60	285.33	179.53	11,808.00	11,525.50	8.90	34,556.53	+7.54
	Q2	8.20	32.30	430.97	1,045.23	9,601.67	304.67	201.00	11,580.00	11,822.67	8.30	34,994.51	+7.29
	Q3	8.20	32.50	357.90	846.60	7,940.66	250.33	175.73	8,704.80	10,544.30	9.90	28,830.22	+7.14
	Q4	8.30	34.10	514.47	1,027.03	9,458.33	325.50	181.07	11,417.43	11,695.00	8.10	34,626.93	+7.60
	Q5	8.40	36.70	523.53	1,147.67	9,919.33	480.00	184.37	10,695.30	12,339.77	6.50	35,296.47	+7.86
	Q6	7.80	34.80	394.00	1,131.33	9,549.65	289.00	192.13	10,453.00	12,305.67	18.50	34,333.28	+7.62
	Q7	8.20	34.40	453.33	1,238.73	10,165.68	282.67	159.90	12,392.00	12,092.00	7.50	36,791.81	+7.67
	Q8	8.30	35.40	329.40	1,177.33	12,124.70	386.67	156.45	12,387.00	12,278.33	6.01	38,845.89	+7.81
	Q9	8.30	36.70	483.83	1,267.17	9,949.00	300.00	156.33	12,376.00	12,317.10	5.90	36,855.33	+7.95
	Q10	8.30	36.80	496.97	1,237.50	10,162.60	296.67	166.10	13,461.33	12,415.10	6.40	38,242.67	+7.93
	Q11	8.30	37.00	463.43	1,217.33	10,887.67	289.83	157.20	13,630.00	12,472.37	6.50	39,124.33	+7.93
	Q12	8.40	36.90	453.20	1,203.00	12,271.00	362.00	157.13	12,207.00	12,383.67	5.50	39,042.50	+7.89
	Q13	8.30	36.60	449.53	1,100.17	10,158.50	296.00	170.73	12,283.33	12,509.37	9.70	36,977.33	+7.79

Water system	Sampling sites	SI Calcite	SI Gypsum	SI Halite
Irrigation waters	1	-0.05	-2.21	-7.91
	2	-0.08	-2.09	-7.50
	3	-0.06	-2.19	-7.87
	4	-0.22	-2.13	-7.69
	5	0.04	-2.10	-7.76
	6	-0.20	-2.22	-7.76

Table 2 continued

Water system	Sampling sites	SI Calcite	SI Gypsum	SI Halite
	7	−0.25	−2.12	−7.45
	8	−0.26	−2.05	−7.41
	9	−0.20	−2.37	−7.99
	10	0.01	−1.93	−7.16
	11	−0.06	−1.88	−7.13
	12	0.04	−1.89	−7.17
	13	0.26	−1.68	−6.82
	14	−0.08	−1.93	−7.18
	15	0.00	−1.70	−6.64
	16	0.43	−1.55	−6.42
	17	0.48	−0.90	−5.06
Drainage waters	18	−0.11	−1.64	−6.46
	19	0.14	−1.47	−6.59
	20	0.21	−1.37	−6.19
	21	0.28	−1.22	−6.08
	22	0.49	−1.17	−6.01
	23	0.72	−0.87	−5.12
	24	0.04	−1.64	−6.46
	25	0.46	−1.27	−5.88
	26	0.28	−1.03	−5.83
	27	0.20	−1.09	−5.85
	28	0.17	−1.07	−5.80
	29	0.36	−0.91	−5.15
Lake Qarun waters	Q1	0.81	−0.07	−2.83
	Q2	0.89	−0.07	−2.80

Table 2 continued

Water system	Sampling sites	SI Calcite	SI Gypsum	SI Halite
	Q3	0.79	−0.20	−2.93
	Q4	0.98	0.01	−2.81
	Q5	1.05	−0.01	−2.76
	Q6	0.49	−0.14	−2.78
	Q7	0.80	−0.04	−2.77
	Q8	0.71	−0.19	−2.69
	Q9	0.90	−0.01	−2.77
	Q10	0.92	0.02	−2.76
	Q11	0.90	−0.02	−2.74
	Q12	0.90	−0.06	−2.68
	Q13	0.88	−0.05	−2.76

Units are in mg/L, except EC (mS/cm), pH, $\delta^{18}O$, and saturation index (SI)

[a] Average values of water samples collected during June 2010, 2011, and 2012 from Lake Qarun (Q1–Q13) and from El-Wadi and El-Bats drains outlets (samples 23 and 29, respectively)

[b] $\delta^{18}O$ was measured only during June 2012

3 Results and Discussion

The physiochemical results of the investigated water samples are presented in Table 2. The data showed that the TDS trend increases from the head of Fayoum irrigation system at sampling site 1 toward Lake Qarun (Fig. 4). In general, the concentrations of most ions and TDS are in the order; lake water ≫ drainage water > irrigation water (Table 2). Only one sample (sampling site 17) from irrigation canals was found to have a TDS value of 2,350.37 mg/L, which is more than the TDS of drainage waters (Table 2). This is because the water depth was very shallow when this sample was taken during sampling and also the water flowed for a long distance from sampling site 1 to sampling site 17. Therefore, water salinity increased by evaporation. Sample 17 has the highest value of $\delta^{18}O$ (+4.22) among all irrigation waters and drainage waters (Table 2). The $\delta^{18}O$ is concentrated in water as a result of evaporative concentration (Gat 1996).

According to the spatial distribution of TDS values of Fayoum surface waters, it was found that water salinity increases with increasing proximity to Lake Qarun (Fig. 4). In Lake Qarun, it is noted that the TDS of the lake water is low at the eastern part and gradually increases north-westward. This could be due to the dilution effect of drainage water discharging into the lake from the southeastern side rather than the northwestern. The effect of dilution is observed near the outlet mouths of El-Bats and El-Wadi drains which have lower TDS than the other sites in the lake (Fig. 4).

3.1 Hydrochemical Water Types

Chadha (1999) developed a new diagram for geochemical classification of natural waters and interpretation of chemical data. In this diagram, the difference in milliequivalent percentage between alkaline earth (Ca + Mg) and alkali metals (Na + K) is plotted on the X axis, and the difference in milliequivalent percentage between weak acidic anions
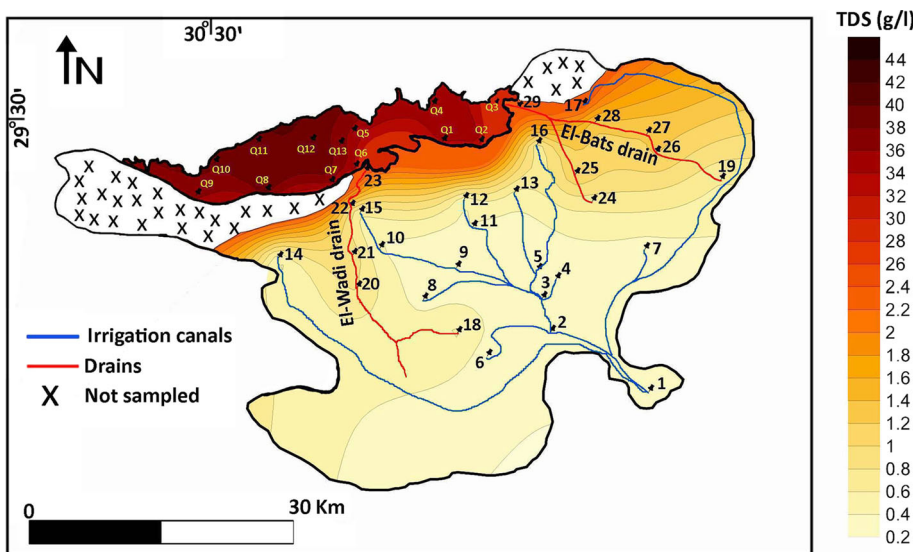
Fig. 4 Spatial distribution of TDS on the studied area showing that salinity increases with increasing proximity to Lake Qarun

Fig. 5 Chadha diagram showing the hydrochemical water types of the studied water samples (Chadha 1999)
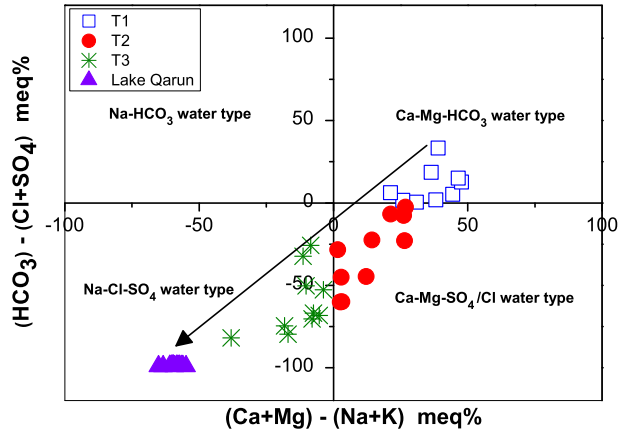
$(CO_3 + HCO_3)$ and strong acidic anions $(Cl + SO_4)$ plotted on the Y axis. Plotting of the studied water samples on the diagram revealed the presence of three hydrochemical water facies: water type 1 (T1), water type 2 (T2) and water type 3 (T3) (Fig. 5).

3.1.1 Water Type 1 (T1): (Ca–Mg–HCO₃)

This type is mainly irrigation water, collected from sites 1–9 close to the head of Fayoum irrigation system (Fig. 1). These waters are almost always fresh with minimum TDS (248.52 mg/L) at sampling site 9 and maximum TDS (336.33 mg/L) at sampling site 8. The waters of T1 type are slightly alkaline (pH 7.50–7.77, Table 2). This water type is characterized by higher concentrations of weak acidic anions mainly HCO_3 than strong acidic anions $(Cl + SO_4)$ (Fig. 5). It also has higher concentrations of alkali earth elements $(Ca + Mg)$ than alkali metals $(Na + K)$. All waters of T1 type are undersaturated with respect to calcite except only one sample (sample 5) is just at saturation (Table 2; Fig. 6). All T1 waters are undersaturated with respect to gypsum and halite (Fig. 6).

3.1.2 Water Type 2 (T2): (Ca–Mg–SO₄/Cl)

This water type includes samples 10, 11, 12, 13, 14, 15, 16, 19, 21, and 22. These water samples are characterized by higher concentrations of strong acidic anions $(Cl + SO_4)$ than weak acidic anions mainly HCO_3 and higher concentrations of alkali earth elements $(Ca + Mg)$ than alkali metals $(K + Na)$ (Fig. 5). Water type (T2) includes both irrigation waters (sampling sites 10–16) and drainage waters (sampling sites 19, 21 and 22) (Fig. 1). The T2 waters are much closer to Lake Qarun than those of T1 (Fig. 1). The TDS of T2 waters collected from irrigation canals ranges from 419.44 mg/L (sample 10) to 676.54 mg/L (sample 16) while it ranges from 616.54 mg/L (sample 19) to 1,064.14 mg/L (sample 22) for samples collected from drainage waters (Table 2). The waters of type T2 have pH ranges 7.50–7.90 (Table 2). Most of T2 waters are supersaturated with respect to calcite except two samples; samples 11 and 14 are still undersaturated (Table 2; Fig. 6). All T2 waters still undersaturated with respect to gypsum and halite (Fig. 6).

Fig. 6 Calculated saturation indices of **a** calcite, **b** gypsum, and **c** halite of the studied water samples. All saturation indices increase toward Lake Qarun due to the effect of the evapoconcentration process
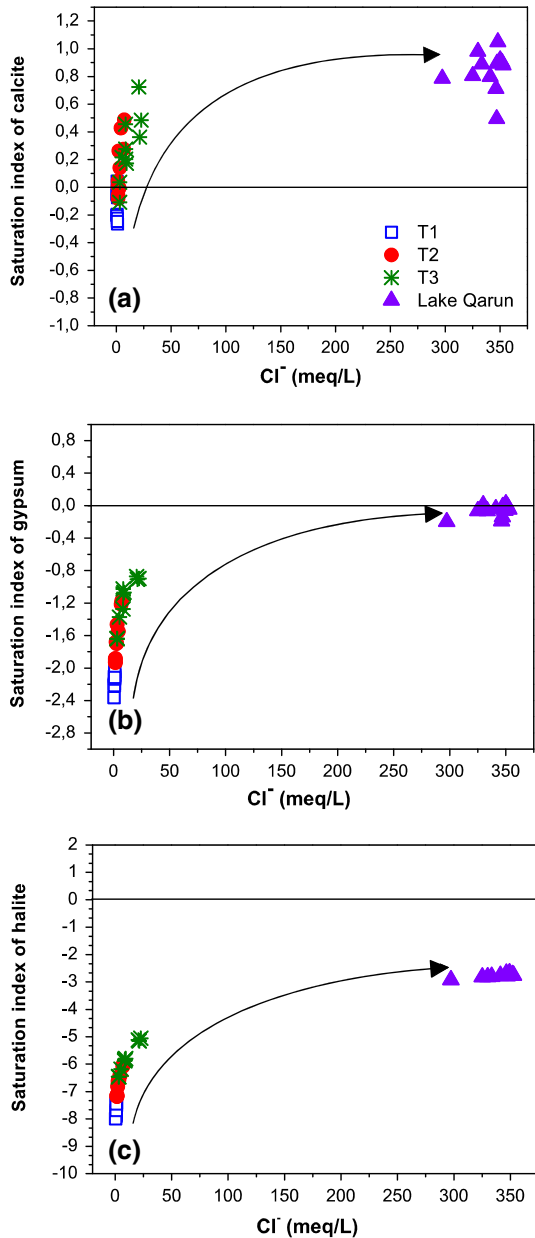
3.1.3 Water Type 3 (T3): (Na–Cl–SO₄)

This water type includes water samples collecting from sites 17, 18, 20, 23, 24, 25, 26, 27, 28, and 29. All of these water samples were taken from drains except sample 17 which was taken from an irrigation canal. All drainage waters are conveyed into the two main drains, El-Wadi and El-Bats. Water samples 23 and 29 were collected from the outlet mouths of

El-Wadi and El-Bats drains, respectively, which represent the main inputs of drainage water to Lake Qarun (Fig. 1). Samples 23 and 29 have the highest salinities among all drainage waters (2,283.30 and 2,172.24 mg/L, respectively). On the other hand, sample 17 has the highest salinity (2,350.37 mg/L) between all irrigation and drainage waters that were collected from Fayoum (Table 2; see also Sect. 3). All waters of T3 type are characterized by higher concentrations of strong acidic anions ($Cl + SO_4$) than weak acidic anions mainly HCO_3 and higher concentrations of alkali metals ($K + Na$) than alkali earth elements ($Ca + Mg$) (Fig. 5). The pH of T3 water type ranges from 7.50 to 7.70. All T3 waters are supersaturated with respect to calcite except only one sample (sample 18) is still undersaturated (Table 2; Fig. 6). On the other hand, all T3 waters are undersaturated with respect to gypsum and halite (Fig. 6).

3.1.4 Lake Qarun Water; (Na–Cl–SO₄)

Lake Qarun water samples lie in the field of T3 water type. They are characterized by very high TDS values and high pH values as compared to the irrigation and drainage waters (Table 2). The highest TDS recorded at site Q11 with value 39,124.33 mg/L and the highest pH recorded at sites Q5 and Q12 with value 8.40 for both samples. The lake water is supersaturated with respect to calcite at all locations (Fig. 6). On the other hand, only two locations in Lake Qarun (Q4 and Q10) just reached the saturation state with respect to gypsum while the other locations still undersaturation (Table 2; Fig. 6). The lake water still undersaturation with respect to halite at all locations (Fig. 6).

3.2 Geochemical Evolution of Irrigation and Drainage Waters in the Fayoum Depression

The geochemical alteration of the Nile water (main source of fresh water) through its course along Fayoum Depression is the main concern of this section. As shown in Chadha diagram (Fig. 5), the surface water in Fayoum Depression have evolved from Ca–Mg–HCO₃ water type (T1) at the head of Fayoum irrigation system to the Na–Cl–SO₄ water type (T3) close to and at Lake Qarun passing through a transitional Ca–Mg–SO₄/Cl water type (T2). The HCO_3^- decreases proportionally relative to Cl^- and SO_4^{2-}, and also Ca^{2+} and Mg^{2+} decrease proportionally relative to Na^+ with increasing proximity to Lake Qarun (Fig. 5).

Yan et al. (2002) concluded that weathering of carbonate rocks leads to freshwaters low in dissolved silica (<20 mg/L) with a SiO₂/HCO₃ molar ratio 0.02. Also, ternary plots of cations (Na + K − Mg − Ca) as well as anions (Cl + SO₄ − HCO₃ − Si) could explore the relative importance of different weathering regimes (Stallard and Edmond 1981). Accordingly, the T1 waters have SiO₂ ranges 4.53–6.23 mg/L (Table 2) with an average SiO₂/HCO₃ molar ratio equal to 0.04 (calculated from Table 2), and they fall in the cluster toward HCO₃ and Ca apexes (Fig. 7). This suggests that weathering of carbonates is the dominant process contributing to this water type. All T1 waters are undersaturated with respect to calcite (Fig. 6a). Limestone which is composed mainly of calcite is abundant at the studied area. Consequently, congruent dissolution of calcite should give Ca/HCO₃ molar ratio equals to 0.5 as shown in the following reaction:

$$\underset{\text{Calcite}}{CaCO_3} + H_2O + CO_2 \rightarrow Ca^{2+} + 2HCO_3^- \tag{1}$$
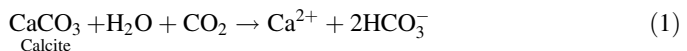
The plotting of Ca^{2+} versus HCO_3^- showed that all samples fall close to the 1:2 line with some points having little excess of HCO_3^- (Fig. 8). The influx of CO_2 that might be
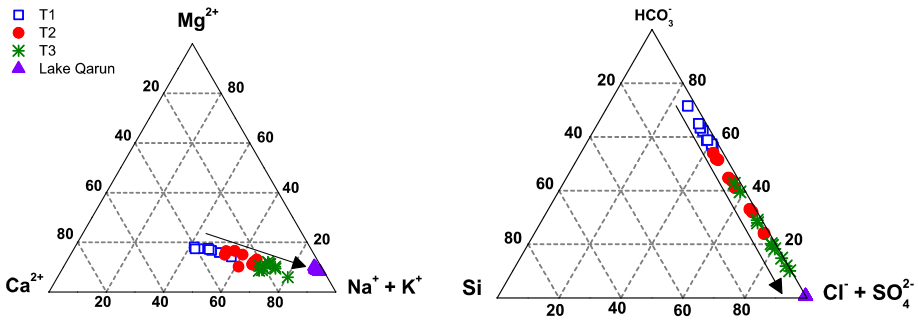
Fig. 7 Ternary diagram showing the chemical trends of the studied water samples (in mmol%). The points have evolved from HCO_3^- apex to Cl^- and SO_4^{2-} apexes and from Ca^{2+} and Mg^{2+} apexes to $Na^+ + K^+$ apex as water flows toward Lake Qarun

Fig. 8 Binary plot of Ca^{2+} versus HCO_3^- of T1 waters. Most of T1 waters lie close to the 1:2 line
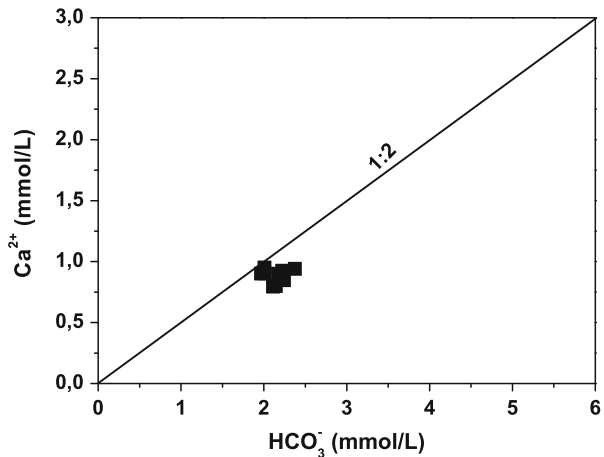
released by the decay of organic materials can be mobilized and takes part in chemical reactions (Hem 1986). If it is assumed that each CO_2 molecule could react with solid CO_3 to give two HCO_3^- ions (Eq. 1), reactions with noncarbonate minerals would yield one HCO_3^- ion for each participating CO_2 molecule which could contribute to the little excess HCO_3^- over Ca^{2+} in T1 waters (Hem 1986).

As the surface water flows toward Lake Qarun, waters of T2 and T3 types have evolved from T1 type with an increase of Cl^- and SO_4^{2-} relative to HCO_3^- along with an increase of Na^+ relative to Ca^{2+} and Mg^{2+} (Figs. 5, 7). The colocation of Na^+, Cl^-, and SO_4^{2-} can be explained by the fact that various evaporites are present in the studied area (Huang et al. 2009). Gypsum is abundant in the current studied area (Fayoum Depression). Also, gypsum is added to improve Fayoum soil productivity especially to the lands close to the southern shore of Lake Qarun. These lands cover an area of 198 km² and are classified as highly saline and poor productivity soils (Abdel Kawy and Belal 2013). In addition, most lacustrine and alluvial–lacustrine soils in the Fayoum Depression are actually degraded by salinization. Salts crusts on the soil surfaces are observed during hot and dry conditions in summer. Most of the drainage and irrigation waters samples of T2 and T3 lie in the regions

of lacustrine and alluvial–lacustrine soils which are rich in gypsum and soil salts. As a result, congruent dissolution of soluble minerals such as gypsum ($CaSO_4 \cdot 2H_2O$) or halite (NaCl) from these types of soils can lead to very high Na^+, SO_4^{2-}, and Cl^- concentrations in T2 and T3 waters (Eugster 1980). Also, the subsequent leaching of readily soluble salts (e.g., NaCl) from the soil surface progressively increases the salinity of the surface water and raises the level of Na^+ and Cl^- in the agricultural returns.

Mineral equilibrium and saturation indices calculations could predict the reactive mineralogy (Deutsch 1997). The SI of calcite, gypsum, and halite for all the studied water samples is given in Fig. 6. The results showed that waters of T1 are undersaturated with respect to calcite, gypsum, and halite. Close to Lake Qarun, most waters of T2 and T3 types became supersaturated with respect to calcite and still undersaturated with respect to gypsum and halite (Fig. 6). Therefore, the dissolution of gypsum and halite is expected to contribute to the solute budget of T2 and T3 waters. As the saturation state indicates the direction of the process, precipitations of carbonate minerals accompanied by the dissolution of evaporites such as gypsum and halite possibly have influenced the chemical evolution of water from $Ca–Mg–HCO_3$ at locations of T1 type to $Na–SO_4–Cl$ at locations of T3 passing through a transitional $Ca–Mg–SO_4/Cl$ at locations of T2 (Figs. 5, 6, 7).

To verify the contribution of gypsum and halite dissolution to T2 and T3 waters, binary plotting of $[(Ca^{2+} + Mg^{2+}) - 0.5\ HCO_3^-]$ against SO_4^{2-} and also Na^+ against Cl^- were studied. The contribution of gypsum to the concentration of Ca^{2+} can be estimated by studying the relationship between the noncarbonate mineral-derived Ca and Mg using the formula $[(Ca^{2+} + Mg^{2+}) - 0.5\ HCO_3^-]$ plotted against SO_4^{2-} (Kimblin 1995). The binary plotting of $[(Ca^{2+} + Mg^{2+}) - 0.5\ HCO_3^-]$ against SO_4^{2-} for all irrigation and drainage waters showed strong positive correlations $R^2 = 0.969$ and $R^2 = 0.785$ for T2 and T3, respectively, while in the case of T1 showed a weak correlation $R^2 = 0.039$ (Fig. 9). As a result, the dissolution of gypsum probably influences the chemistry of T2 and T3 waters and not influences T1 waters. In the presence of HCO_3^-, the Ca^{2+} ion supplied by gypsum dissolution increases the ion activity product $(a_{Ca}^{2+} + a_{CO3}^{2-})$ and subsequently
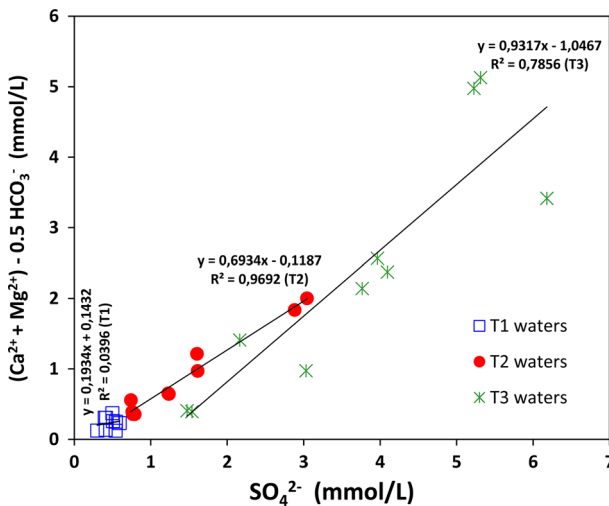
Fig. 9 Binary Plot of $(Ca^{2+} + Mg^{2+}) - 0.5\ HCO_3^-$ against SO_4^{2-} of irrigation and drainage waters in Fayoum Depression shows the contribution of gypsum dissolution to T2 and T3 waters
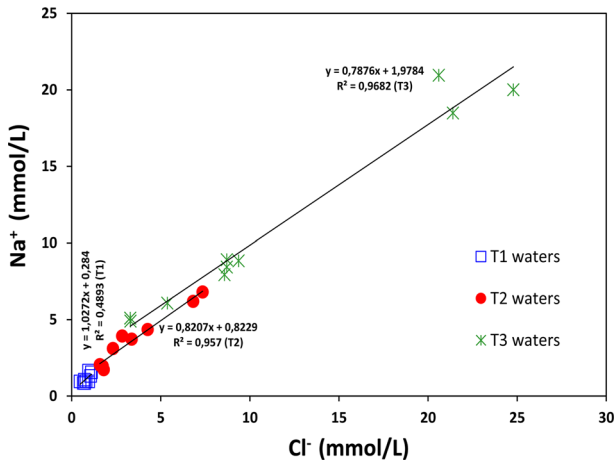
Fig. 10 Binary plot of Na^+ versus Cl^- of irrigation and drainage waters showing the significant dissolution effect of NaCl salt on T2 and T3 waters

increases the saturation index of calcite (Dargam and Depetris 1996). This process may explain why the saturation state with respect to calcite changed from undersaturation in the case of T1 to supersaturation for T2 and T3 waters (Fig. 6).

The binary plotting of Na^+ against Cl^- for all irrigation and drainage waters showed strong positive correlations in the case of T2 waters ($R^2 = 0.957$) and T3 waters ($R^2 = 0.968$) while in the case of T1 showed a weak correlation ($R^2 = 0.480$) (Fig. 10). This indicates that halite dissolution has significantly impacted the chemical composition of T2 and T3 waters.

The contribution of evaporite dissolution to T2 and T3 waters is also evidenced in the ternary plot where the irrigation and drainage waters of T2 and T3 fall in the cluster toward Na + K apex and Cl + SO_4 apex (Fig. 7).

3.3 Hydrogeochemical Evolution of Lake Qarun

Lake Qarun water has a Na–SO_4–Cl water type (Fig. 5). T3 waters specially samples 23 and 29, which represent the outlet mouths of El-Wadi and El-Bats drains, respectively, have the same Na–SO_4–Cl water type like Lake Qarun (Fig. 5). As mentioned previously, El-Bats and El-Wadi drains represent the main sources of drainage water recharge to Lake Qarun (Fig. 1). Thus, Lake Qarun as a closed system seems to be evolved geochemically from drainage water inflow as a result of progressive evaporation. Gibbs (1970) suggested a simple plot of TDS versus the weight ratio of $Na^+/(Na^+ + Ca^{2+})$ could provide information on the relative importance of the major natural mechanisms controlling surface water chemistry (Fig. 11). In the present study, a Gibbs plot of data indicates that T1 and T2 water chemistry are mainly controlled by rock weathering. Some of T3 waters lie in the rock weathering domain while others are controlled by evaporation-crystallization process. This supports the earlier suggestions that weathering of carbonates controls the chemistry of T1 waters while T2 and T3 waters are controlled by weathering of evaporites. Some waters of T3 lie on the field of evaporation crystallization perhaps due to the fact that much of the evaporation can be ascribed to the use of water for irrigation, where a greater surface
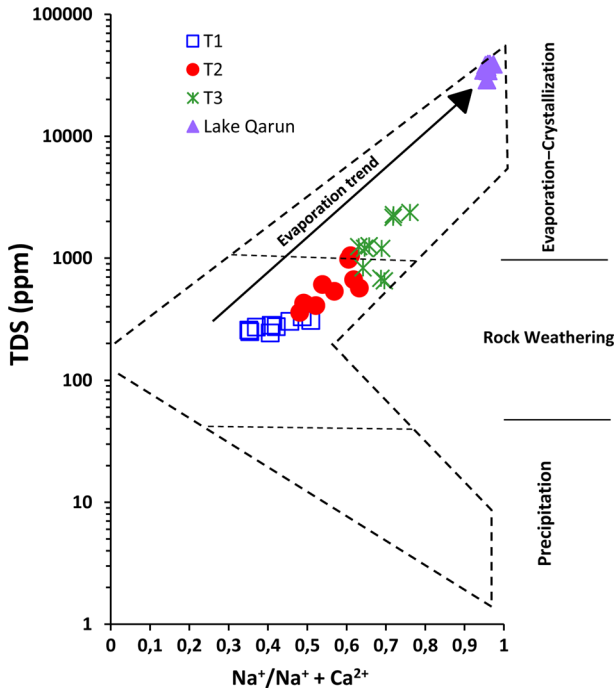
Fig. 11 Gibbs plot showing the mechanisms controlling the major ion composition of the surface water in Fayoum Depression. Lake Qarun water is mainly controlled by evaporation-crystallization process

area of water is made available for evaporation before the remaining water is returned to drains as drainage waters (agriculture returns). Also, intensive agriculture practicing can increase the weathering and erosion of soil salts resulting in a higher TDS of the agriculture returns. Lake Qarun water is characterized by a high Na/(Na + Ca) ratio and a high TDS concentration, suggesting that it is mainly controlled by an evaporation-crystallization process (Fig. 11). The chemical composition of surface water in Fayoum Depression evolves (in a sequence of water samples taken in a Lake Qarun direction) from rock-weathering-type waters found in headwaters to more concentrated sodic waters found in Lake Qarun as a result of evaporation and concentration of salts accompanied by the crystallization of $CaCO_3$. This is most likely because the saturation index of calcite evolves from undersaturation state in headwaters (T1) to supersaturation state in Lake Qarun (Fig. 6). The hot and dry climatic conditions prevailed throughout the area strengthen the evaporation trend from head waters to Lake Qarun that clearly obvious on Gibbs's model (Fig. 11). Thus, under arid conditions, the continuous evaporation under a very long span of time leads to a dramatic effect in the water chemistry of Lake Qarun, resulting in the higher levels of Na^+ and Cl^- than those found in the transition and upstream areas as well as a drastic increase in the TDS of the lake water (Fig. 11). In the ternary plot (Fig. 7), Lake Qarun waters plotted very close to the Na + K and Cl + SO$_4$ apexes. In Lake Qarun, HCO_3^- decreases proportionally relative to Cl^- and SO_4^{2-} while Ca^{2+} and Mg^{2+} decrease proportionally relative to Na^+ (Figs. 5, 7). The increase of Na^+, Cl^-, and SO_4^{2-} in Lake Qarun is mainly due to solute accumulation by evaporation while the depletion of Ca^{2+} and HCO_3^- could be due to carbonate mineral precipitation.

All saturation indices of calcite, gypsum, and halite increase with increasing proximity to Lake Qarun and the highest values recorded in the lake itself (Fig. 6). This indicates that continuous water loss by evaporation in Lake Qarun causes the increase in concentration of these minerals.

3.4 Application of Hardie and Eugster's Model

Hardie and Eugster (1970) suggested a model that interprets the chemistry of waters undergoing evaporation in terms of a succession of chemical divides. A chemical divide is a point in the evolution sequence of brine in which precipitation of a mineral depletes the water in certain cations or anions with further evaporation moves the solution along a distinct pathway. This was called "fractionation by mineral precipitation" (Eugster 1980) or principle of chemical divide as described by Drever (1982) and is now popularized under the name of "chemical divide" (Bąbel and Schreiber 2014). The main idea of the principal of chemical divide is that molar ratio of the component ions of precipitated salt must change, unless it is exactly equal to one in the initial solution at the beginning of evaporation process (Bąbel and Schreiber 2014; Drever 1982). Therefore, the ion with the lower concentration at the onset of evaporitic precipitation will progressively decrease in concentration, whereas the other ion showing initially higher concentration will build up in solution. The Hardie and Eugster's model has been simply modified by Drever (1982) (Fig. 12). This modified model is obviously very simple, and it is generalized to cover a wide range of starting compositions of the water to be evaporated. With almost of natural waters, the first mineral to precipitate, and hence to cause the first chemical divide, is calcite (Drever 1982). Further evaporation moves the solution along path I or path II depends on whether the calcium concentration (in equivalents) is greater or less than the carbonate alkalinity (in equivalents) (Fig. 12). In almost of natural waters, the alkalinity is mainly expressed as HCO_3^- (Eugster 1980; Eugster and Hardie 1978). In the present case, close to the head of the Fayoum irrigation system, the waters of type T1 (samples 1–9) have $2mCa^{2+} < mHCO_3^-$ on average. The total average of $mHCO_3^-$ of T1 waters is
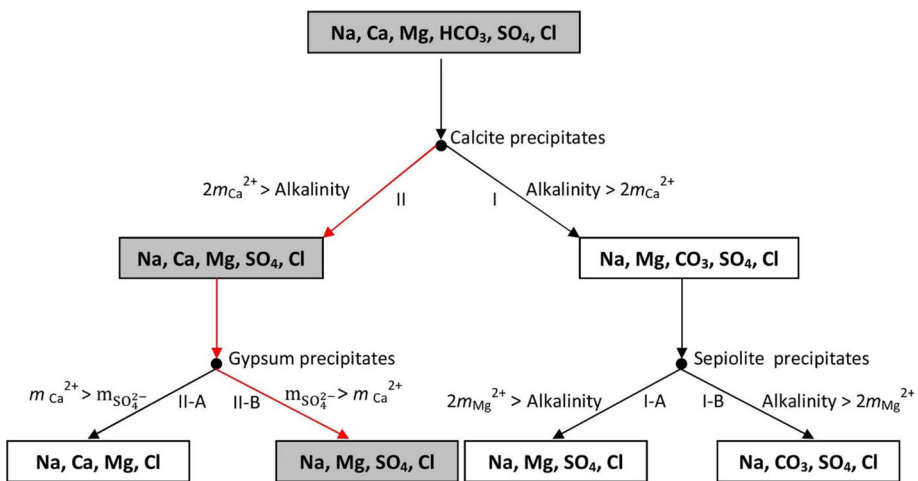
Fig. 12 Some possible paths during evaporation of natural water (a model modified from Hardie and Eugster 1970 by Drever 1982). Lake Qarun water should evolve along the path II–IIB
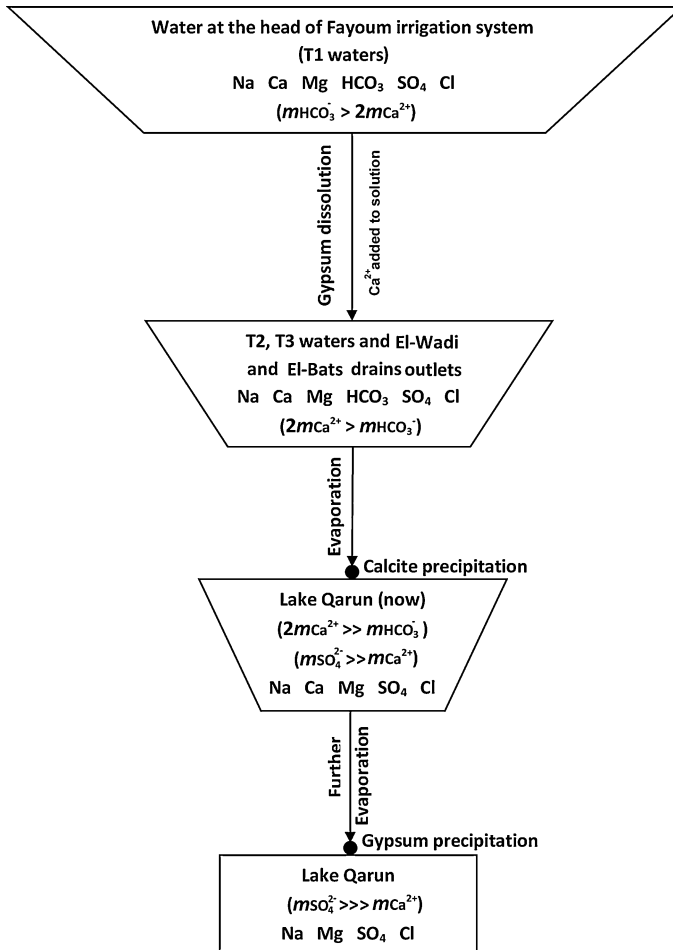
Fig. 13 Suggested flow chart shows the possible path for the geochemical evolution of surface water in Fayoum Depression

2.14 mmol/L while the total average of $2m\text{Ca}^{2+}$ is 1.77 mmol/L (calculated from data in Table 2). This initial composition, during evaporation, should force the solution to follow path I (Fig. 12). But, along the flow path of surface water toward Lake Qarun, the Ca^{2+} supplied by gypsum dissolution produced a significant increasing of the $2m\text{Ca}^{2+}/m\text{HCO}_3^-$ ratio (Fig. 13). As a result, the average composition of water turned from $2m\text{Ca}^{2+} < m\text{HCO}_3^-$ at the head of the Fayoum irrigation system (T1 waters) to $2m\text{Ca}^{2+} > m\text{HCO}_3^-$ in low lands at T2 and T3 waters (Fig. 13). The calculated average of $2m\text{Ca}^{2+}$ for all T2 and T3 waters became 4 mmol/L while $m\text{HCO}_3^-$ became 3.1 mmol/L (calculated from data in Table 2).

Furthermore, the drainage waters at El-Wadi and El-Bats drains outlets (samples 23 and 29, respectively), which represent the main sources of surface water to Lake Qarun, have also an average $2m\text{Ca}^{2+} > m\text{HCO}_3^-$ with an average $2m\text{Ca}^{2+}$ equal to 5.6 mmol/L and an average $m\text{HCO}_3^-$ of 3.3 mmol/L (calculated from data in Table 2).

As discussed above, the drainage waters at El-Wadi and El-Bats drains outlets, as the main inflow to Lake Qarun, have a $2m\text{Ca}^{2+} > m\text{HCO}_3^-$. During evaporation, this solution

should follow path II (Fig. 12). In Lake Qarun, calcite precipitation (the first chemical divide) causes Ca^{2+} to build up in solution while HCO_3^- diminishes and the lake water progressively evolved to $2mCa^{2+} \gg mHCO_3^-$ (Fig. 13; Table 2). On path II, the next mineral that is most likely to precipitate is gypsum, which causes the second chemical divide (Fig. 12). Further evaporation will force the solution to move along path IIA or path IIB depends on whether the Ca^{2+} concentration is greater or lesser than the concentration of SO_4^{2-} (Fig. 12). The current status of Lake Qarun water is $mSO_4^{2-} \gg mCa^{2+}$ with an average mSO_4^{2-}/mCa^{2+} ratio of lake water is ≈ 11 (calculated from data in Table 2). This means the solution will follow path IIB (Fig. 12). The precipitation of gypsum will produce $mSO_4^{2-} \ggg mCa^{2+}$ because of the initial excess of SO_4^{2-} over Ca in lake water (Fig. 13). Continuous precipitation of gypsum will remove Ca^{2+} while SO_4^{2-} will build up in solution until lake water reaches the final composition "Na–Mg–SO_4–Cl" (Figs. 12, 13). At some locations of Lake Qarun, the water reached saturation state with respect to gypsum (Fig. 6). This suggests that gypsum divide is coming next to calcite divide in Lake Qarun water which supported that the lake water will be evolved along the path II–IIB. Gypsum never appears along path I (Eugster 1980). This also supports our hypothesis that the lake water during its evolution should follow path II rather than path I. Gypsum precipitation will not greatly affect the SO_4^{2-} concentration due to the huge initial excess of SO_4^{2-} over Ca^{2+} in Lake Qarun.

3.5 Behavior of Major Ions During Evaporation of Lake Qarun Water

Water in endorheic lakes in arid and semiarid areas often becomes saline or hypersaline as a result of evaporative enrichment (Fritz 1990). To study the behavior of major solutes during lake water evolution, the concentrations of the major ions (in meq/L) are plotted against chloride (Fig. 14). In most cases, species concentrations are plotted against Cl because chloride once dissolved is assumed to act conservatively until halite precipitation and also to indicate the degree of up-concentration of solutes in the waters, either due to evaporite dissolution or to evapotranspiration (Banks et al. 2004; Smith and Compton 2004). It appears that concentrations of major ions such as Na^+, Mg^{2+}, and Ca^{2+} and SO_4^{2-} as a function of Cl^- are building up in solution by evapoconcentration (Fig. 14). Only HCO_3^- shows depletion against Cl^- during evaporation (Fig. 14a). The HCO_3^- might be removed from Lake Qarun due to precipitation of calcite. The Ca^{2+} concentration in lake water does not show depletion against Cl^- throughout calcite precipitation (Fig. 14b). This is due to the relative initial excess of Ca^{2+} over HCO_3^- in the lake water. Thus, calcite precipitation in Lake Qarun is limited by HCO_3^-. Additionally, removal of Ca^{2+} through gypsum precipitation is possibly not observably achieved. This is due to the fact that only few locations in Lake Qarun just reached saturation with respect to gypsum (Fig. 6). This means gypsum is currently not precipitating in Lake Qarun with huge amounts because it did not reach the supersatuartion state yet. Also, waters do not start to precipitate gypsum until they are nearly free of HCO_3^- (Hardie and Eugster 1970).

3.6 Simulation Model of Evaporation Trend of Lake Qarun Water

The concept of this model is to predict the changes in lake water chemistry by any further evaporation. If the rate of evaporation at the area of Lake Qarun will be constant like the present time, the predicted decreasing of water flow from Nile River to Lake Qarun after construction of the Ethiopian Dam can cause a negative value in the lake water storage. However, the predicted climatic changes via global warming can led to higher rates of
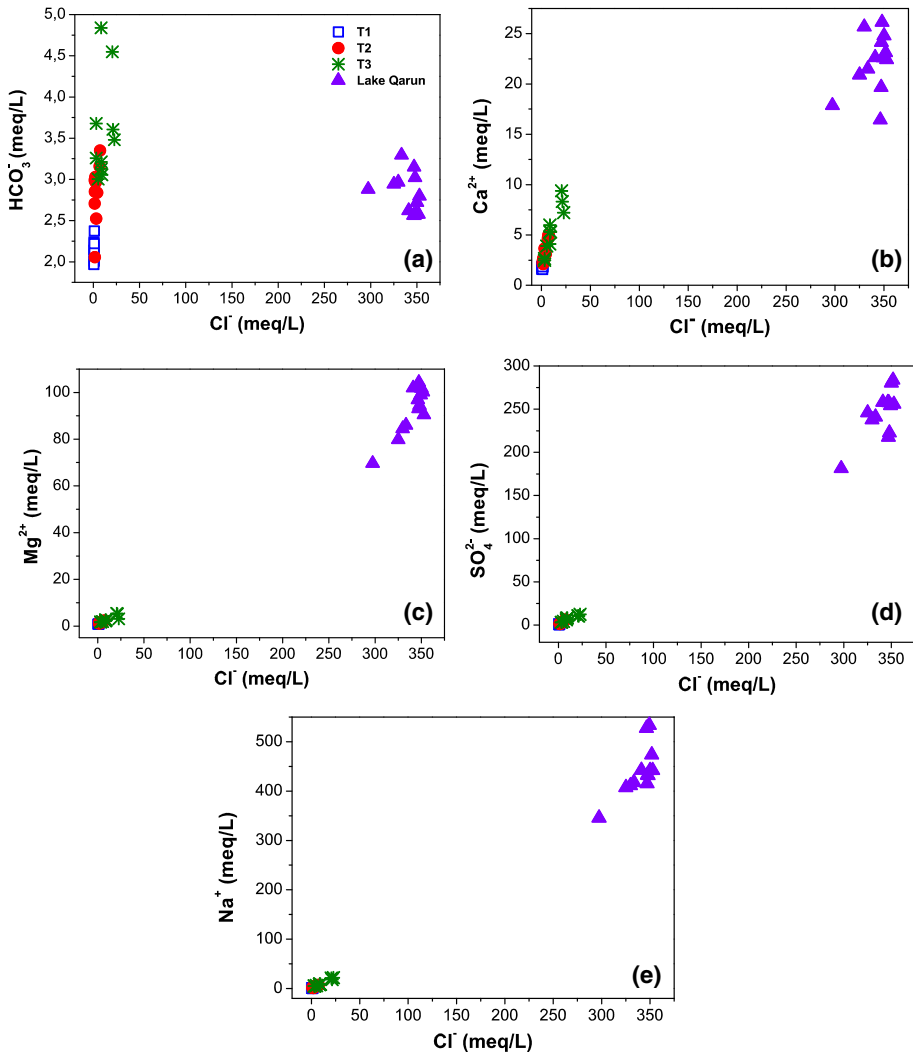
Fig. 14 Concentrations of **a** HCO₃, **b** Ca, **c** Mg, **d** SO₄, and **e** Na plotted against Cl for sampled waters. All ions in Lake Qarun increase with increasing Cl except HCO₃ which removed as a result of CaCO₃ precipitation

evaporation than the current situation. So, in future, a further evaporation of lake water is expected, and this will modify the geochemical behavior of lake water. Abdel Wahed et al. (2014) studied a simulated evaporation model of drainage water inflow toward Lake Qarun. They stated that the lake water has been evolved from the surface drainage water mainly by evapoconcentration process through which HCO_3^- removed by calcite precipitation and lake water just reached saturation state with respect to gypsum and still undersaturated with respect to halite. These findings by were correlated very well with the real composition of Lake Qarun water (Abdel Wahed et al. 2014).

Currently, Lake Qarun water is supersaturated with respect to calcite, saturated with respect to gypsum at some locations, and undersaturated with respect to halite at all

locations (Fig. 6). Also, HCO_3^- depleted during calcite precipitation (Fig. 14). What is the expected evolution of Lake Qarun water under further evaporation? To answer this question, a simulated evaporation model was carried out. In the present study, the simulated evaporation model was carried out at a constant partial CO_2 pressure of $10^{-3.5}$ and temperature of 25 °C. Also, whenever the water became saturated with respect to calcite, gypsum, or halite, these solid phases will precipitate and the solution will remain in equilibrium with them. The model was simulated using PHREEQC-3 software program with Pitzer database (Parkhurst and Appelo 2013). The simulated model was designed to simulate the evaporative concentration of the 1 L of water by the removal of 52.5 mol of water in 20 steps (i.e., 94.6 % of water removed). The output results of the simulated model will be compared with the Hardie and Eugster's model that was described earlier. As it is mentioned earlier, Lake Qarun water during evaporation should follow the path II–IIB (Figs. 12, 13) along which calcite and gypsum should precipitate and the water reaches the final composition "Na–Mg–SO_4–Cl" (neutral brine). Along the path II–IIB, calcite precipitation is limited by HCO_3^- while gypsum precipitation is limited by Ca^{2+}. Calcite precipitation is already observed in Lake Qarun. On the other hand, the lake water did not show depletion of Ca^{2+} as a result of gypsum precipitation. This is because only few locations in the lake are just reached the saturation state with respect to gypsum. However, because the lake water reached the saturation state with respect to gypsum, this means that any further evaporation of lake water should force gypsum to precipitate. Thus, during further evaporation through the simulated evaporation model, removal of Ca^{2+} from solution is expected due to precipitation of gypsum.

The simulated evolution of major ions species (in mol/kg$_{water}$) and also saturation indices of calcite, gypsum, and halite plotted against Cl^- are shown in Fig. 15. During further evaporation of Lake Qarun water, major species such as Mg^{2+}, Na^+, SO_4^{2-}, and Cl^- should build up in solution, while Ca^{2+} should be removed due to gypsum precipitation (Fig. 15a). Also, the simulated saturation indices results showed that calcite and gypsum are precipitated and became in equilibrium with the solution during the further evaporation of lake water (Fig. 15b). Calcite precipitation is limited by HCO_3^- while gypsum precipitation is limited by Ca^{2+}. On the other hand, the solution reached supersaturation with respect to halite only at the last step of evaporation (Fig. 15b). So, removal of Ca^{2+} and accumulation of SO_4 during the simulated evaporation as a result of gypsum precipitation is achieved. These findings agreed well with the Hardie and Eugster's model (Figs. 12, 13), in which gypsum divide coming next to calcite divide during evolution of Lake Qarun water by evaporation. Accordingly, by using this simulated model, it is possible to expect the evolution of Lake Qarun water through time. This can be done by monitoring of climate changes and also the changes in the ionic composition of the lake with time and input these data to the PHREEQC software and carry out the simulated model.

3.7 Stable Oxygen Isotope

Variation in the oxygen isotope composition of water is expected to be a function of evaporative enrichment. Increasing evaporative concentration is reflected by increasing $\delta^{18}O$ (Gat 1996). In the present study, the lowest $\delta^{18}O$ of value +3.09 ‰ was recorded for water sample from sampling location 1, which was taken at Lahun at the head of Fayoum irrigation system (see Fig. 1), and the highest surface water value ($\delta^{18}O = +7.95$ ‰) was recorded from the open water of Lake Qarun (Table 2). Water samples collected from the irrigation canals and drains and from the lake close to El-Bats and El-Wadi drains inflows

Fig. 15 **a** Modeled evaporative concentration of Lake Qarun water in equilibrium with a partial CO_2 pressure of $10^{-3.5}$ atm., using PHREEQC-3. Calcite, gypsum, and halite precipitations are permitted. **b** Evolution of mineral saturation indices of calcite, gypsum, and halite during a simulated evaporation of Lake Qarun water modeled by PHREEQC-3
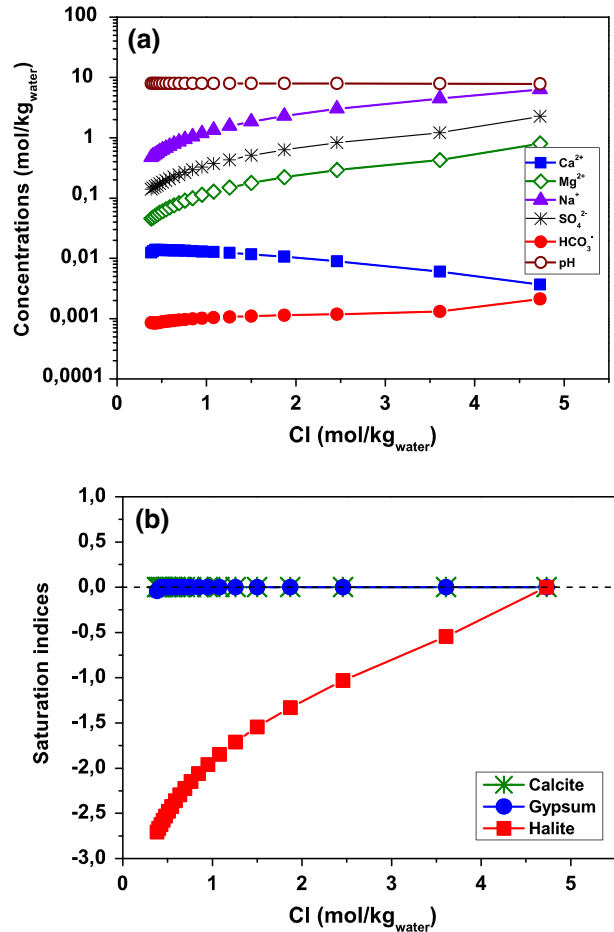
had intermediate values. This suggests that the water is subjected to evaporative concentration as it flows from Lahun to Lake Qarun as evidenced by the resulting $\delta^{18}O$ values. Jusserand et al. (1988) determined the values of $\delta^{18}O$ in the waters of Lake Qarun (sampled in March and August 1984) and discussed their significance and origin. The obtained isotopic values coincide and support the results of the present study.

Given that $\delta^{18}O$ and TDS are largely expected to reflect the degree of evaporation, the rise in the electrical conductivity values of water, from Lahun to the lake, along with the increasing of $\delta^{18}O$, suggests that the water in the Fayoum has been subjected to evaporative concentration. There is a strong positive correlation ($R^2 = 0.99$) between $\delta^{18}O$ and conductivity (Fig. 16), indicating that the rise in $\delta^{18}O$ can be attributed to evaporative concentration. These findings are in good agreement with those of Gibbs's model (Fig. 11), which suggests that the water in Fayoum Depression have been geochemically evolved as a result of evaporative concentration through its course from Lahun toward Lake Qarun. However, the dissolution of preexisting evaporites can contribute to the high TDS concentrations of drainage waters, particularly those collected close to the Lake Qarun. This indicates that the high TDS of drainage waters in Fayoum Depression is possibly due to
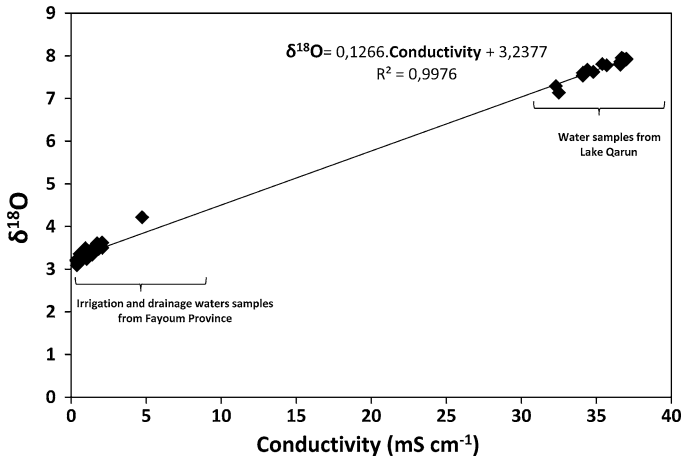
Fig. 16 Relation between $\delta^{18}O$ and conductivity of surface water samples collected from Fayoum Depression. The positive strong correlation reflects the evaporation effect on both TDS and $\delta^{18}O$ values of the surface water in Fayoum Depression

evaporites weathering as well as evapoconcentration process. In some cases of surface runoff with high TDS, it is difficult to distinguish between dissolution of evaporites and evaporation effect on Gibbs's model (Baca and Threlkeld 2000). This is because Gibbs's model (Gibbs 1970) always suggested that the high TDS of surface runoff is controlled only by evaporation. However, both results of $\delta^{18}O$ and Gibbs's model indicate that the Lake Qarun water is mainly controlled by the evaporation-crystallization process (Figs. 11, 16).

4 Conclusion

The geochemical evolution of Lake Qarun water was studied using a number of samples collected from the lake and its surroundings. The sampling plan covered the area's main source of Nile water (water from the Bahr Yousef channel), irrigation waters, drainage water, and lake water. The water evolved along its flow path from Ca–Mg–HCO$_3$ fresh water at the main source, Bahr Yousef, to higher salinity Na–Cl–SO$_4$ drainage waters reaching Lake Qarun. The more saline drainage waters evolve from the initial Bahr Yousef water through processes dominated by the dissolution of evaporite minerals such as gypsum and halite from the Fayoum area and also by evapoconcentration. The dissolution of gypsum leads to increased SO_4^{2-} and Ca^{2+} levels but the high activity of Ca^{2+} in the presence of HCO_3^- forces calcite precipitation, while SO_4^{2-} continues to increase. In contrast, the dissolution of halite increases the Na^+ and Cl^- content of the drainage surface water. Drainage surface waters conveyed by El-Wadi and E-Bats drains represent the main inflow into Lake Qarun. The lake water composition indicates that water in the lake evolved from surface drainage water through progressive evapoconcentration. The application of Hardie and Eugster's model as well as the simulated evaporation model showed that lake water should follow the path on which $2mCa^{2+} > mHCO_3^-$ and then $mSO_4^{2-} > mCa^{2+}$. Along this path, HCO_3^- is removed through calcite precipitation followed by removing of Ca^{2+} through gypsum precipitation and the solution should reach

the final composition "Na–Mg–SO$_4$–Cl." Oxygen isotopes (δ^{18}O) results and Gibbs's model (Gibbs 1970) demonstrated that evaporation crystallization is the main process controlling the evolution of Lake Qarun water chemistry. A simulated evaporation model was carried out to predict the impact of any further evaporation for Lake Qarun water. The model showed that by further evaporation of lake water due to the decrease in water flow to the lake as well as increasing of the rate of evaporation, calcite and gypsum will precipitate within the lake and keep in equilibrium with solution. In addition, lake water reaches supersaturation with respect halite at the latest stages of evaporation. The output results of the simulated model agreed well with the Hardie and Eugster's model and also with the observed ionic composition observed in the water of Lake Qarun.

References

Abdel Kawy W, Belal A (2013) Use of satellite data and GIS for soil mapping and monitoring soil productivity of the cultivated land in El-Fayoum depression, Egypt. Arab J Geosci 6:723–732

Abdel Wahed MSM, Mohamed EA, El-Sayed MI, M'nif A, Sillanpää M (2014) Geochemical modeling of evaporation process in Lake Qarun, Egypt. J Afr Earth Sci 97:322–330

Ali RR, Abdel Kawy WAM (2013) Land degradation risk assessment of El Fayoum depression, Egypt. Arab J Geosci 6:2767–2776

APHA (1998) Standard methods for the examination of water and wastewater. American Public Health Association, Washington

Bąbel M, Schreiber BC (2014) 9.17—Geochemistry of evaporites and evolution of seawater. In: Holland HD, Turekian KK (eds) Treatise on geochemistry, 2nd edn. Elsevier, Oxford, pp 483–560

Baca RM, Threlkeld ST (2000) Inland dissolved salt chemistry: statistical evaluation of bivariate and ternary diagram models for surface and subsurface waters. J Limnol 59:156–166

Baioumy HM, Kayanne H, Tada R (2010) Reconstruction of lake-level and climate changes in Lake Qarun, Egypt, during the last 7000 years. J Great Lakes Res 36:318–327

Ball J (1939) A contribution to the geography of Egypt. Survey and Mines Department, Cairo

Banks D, Parnachev VP, Frengstad B, Holden W, Karnachuk OV, Vedernikov AA (2004) The evolution of alkaline, saline ground- and surface waters in the southern Siberian steppes. Appl Geochem 19:1905–1926

Chadha DK (1999) A proposed new diagram for geochemical classification of natural waters and inter-pretation of chemical data. Hydrogeol J 7:431–439

Dargam RM, Depetris PJ (1996) Geochemistry of waters and brines from the Salinas Grandes basin, Córdoba, Argentina. II. Gypsum dissolution-calcite precipitation, and brine evolution. Int J Salt Lake Res 5:81–101

Deutsch WJ (1997) Groundwater geochemistry: fundamentals and applications to contamination. Lewis Publishers, Florida, Boca Raton

Drever JI (1982) The geochemistry of natural waters. Prentice-Hall, Englewood Cliffs

El-Shabrawy GM, Dumont HJ (2009) The Fayoum depression and its lakes. In: Dumont HJ (ed) The Nile: origin, environments, limnology and human use. Springer, Netherlands, pp 95–124

Eugster HP (1980) Geochemistry of evaporitic lacustrine deposits. Annu Rev Earth Planet Sci 8:35–63

Eugster HP, Hardie LA (1978) Saline lakes. In: Lerman A (ed) Lakes: chemistry, geology, physics. Springer, New York, pp 237–293

Flower RJ, Stickley C, Rose NL, Peglar S, Fathi AA, Appleby PG (2006) Environmental changes at the desert margin: an assessment of recent paleolimnological records in Lake Qarun, Middle Egypt. J Paleolimnol 35:1–24

Fritz SC (1990) Twentieth-century salinity and water level fluctuations in Devil's Lake, N. Dakota: a test of diatom based transfer function. Limnol Oceanogr 35:1771–1781

Gat J (1996) Oxygen and hydrogen isotopes in the hydrologic cycle. Annu Rev Earth Planet Sci 24:225–262

Gibbs RJ (1970) Mechanisms controlling world water chemistry. Science 170:1088–1090

Hammad MA, Abo-El-Ennan SM, Abed F (1983) Pedological studies on the Fayoum area, Egypt, land-scapes and soil morphology. Egypt J Soil Sci 23:99–114

Hardie LA, Eugster HP (1970) The evolution of closed-basin brines. Mineral Soc Am Spec Pap 3:273–290

Hem JD (1986) Study and interpretation of the chemical characteristics of natural water. U.S. Geological Survey Water-Supply Paper 2254

Huang X, Sillanpää M, Gjessing ET, Vogt RD (2009) Water quality in the Tibetan Plateau: major ions and trace elements in the headwaters of four major Asian rivers. Sci Total Environ 407:6242–6254

Jusserand C, Ibrahim AWES, Guelorget O, Perthuisot JP (1988) O^{18} content and salt concentration of lagoonal and continental Egyptian waters. [Teneurs en 18O et concentration saline d'eaux paraliques et continentales égyptiennes]. Rev Sci Water 1(3):277–301

Kimblin RT (1995) The chemistry and origin of groundwater in Triassic sandstone and Quaternary deposits, northwest England and some UK comparisons. J Hydrol 172:293–311

Klein Gebbinck CD, Kim S, Knyf M, Wyman J (2014) A new online technique for the simultaneous measurement of the $\delta^{13}C$ value of dissolved inorganic carbon and the $\delta^{18}O$ value of water from a single solution sample using continuous-flow isotope ratio mass spectrometry. Rapid Commun Mass Spectrom 28:553–562

Meshal AH (1977) The problem of the salinity increase in Lake Qarun (Egypt) and a proposed solution. J Conseil 37:137–143

Metwaly M, El-Qady G, Massoud U, El-Kenawy A, Matsushima J, Al-Arifi N (2010) Integrated geoelectrical survey for groundwater and shallow subsurface evaluation: case study at Siliyin spring, El-Fayoum, Egypt. Int J Earth Sci 99:1427–1436

Parkhurst DL, Appelo CAJ (2013) Description of input and examples for PHREEQC version 3—A computer program for speciation, batch-reaction, one-dimensional transport, and inverse geochemical calculations. US Geological Survey Techniques and Methods, book 6, chap. A43, vol 3, pp 1–504

Rasmy M, Estefan SF (1983) Geochemistry of saline minerals separated from Lake Qarun brine. Chem Geol 40:269–277

Said R (1993) The Nile river: geology, hydrology and utilisation. Pergamon Press, Tarrytown

Smith M, Compton JS (2004) Origin and evolution of major salts in the Darling pans, Western Cape, South Africa. Appl Geochem 19:645–664

Stallard RF, Edmond JM (1981) Geochemistry of the Amazon: 1. Precipitation chemistry and the marine contribution to the dissolved load at the time of peak discharge. J Geophys Res Oceans 86:9844–9858

Tamer AM (1968) Subsurface geology of the Fayoum region. M.Sc. Thesis, Alexandria University

Wolters W, Ghobrial NS, Van Leeuwen HM, Bos MG (1989) Managing the water balance of the Fayoum Depression, Egypt. Irrigat Drain Syst 3:103–123

Yan JP, Hinderer M, Einsele G (2002) Geochemical evolution of closed-basin lakes: general model and application to Lakes Qinghai and Turkana. Sediment Geol 148:105–122